Interrelation of Global Climate and the Response of Oceanic Hydrate Accumulations

Task Report 10-1

Date: January 31, 2011
NETL Manager: Skip Pratt

Principal Investigator: Matthew T. Reagan, mtreagan@lbl.gov, (510) 486-6517

Acknowledgment: "This material is based upon work supported by the Department of Energy."

Using POP bathymetry data, we are establishing a coarse depth-temperature-ΔT map of the oceans, region-by-region, that can used to seed the 1-D, TOUGH+HYDRATE model of dissociation and methane release. These localized assessments are setting the stage for a global coupling (initially one-way, for short term assessment before possible feedbacks would appear) to assess for the first time whether ocean temperature trends are sufficient to inject large amounts of methane into the ecosystem. This report addresses the results of the first basin/regional assessments, and describes the methodology that will drive the larger-scale assessments. In the next step, the basin- and region-scale models are being scaled up to larger assessments, and the regional assessments are being combined to deliver a net global source term of methane, tied to predetermined temperature trends (i.e. IPCC A1B warming values).

The results presented in this report have been presented at the 2010 AGU Fall Meeting and at the 2011 SPE Arctic Technology Conference (Houston, TX, February 7-9) and will be submitted in a peer-reviewed journal in the near future.

Setup of 1-D system

For the basin-scale/regional simulations, we simulate disperse, low-saturation deposits with an initial hydrate saturation, S_{H0}, of 0.03 reflecting the high end of the estimated global average saturation for stratigraphic deposits. We simulate temperature and pressure conditions representing the Sea of Okhotsk and the Beaufort Sea continental shelf from a depth of z = -300 m, above the top of the likely GHSZ for non-permafrost-associated hydrates, to z = -1000 m, a depth at which any hydrates, if present, are expected to not show sensitivity to temperature changes and where short-term temperature changes are expected to be less pronounced. Initial seafloor temperatures range from T_0 = 0.5 ˚C – 1 ˚C, varying with depth, and we assume in nearly all cases a geothermal gradient of 3 ˚C /100m based on the literature.

The representation of each depth/location involves a vertical, 1-D domain describing the sediment column from the seafloor down to z = -360 m, well below the expected range of century-scale temperature perturbations. The initial condition involves a uniform hydrate saturation in the sediment column from the seafloor to the bottom of the GHSZ and a system at complete thermal, chemical, and hydrostatic equilibrium, establishing hydrate distributions, saturations, and aqueous methane concentrations that correspond to the conditions at the selected depth and temperature (see Reagan and Moridis, 2007; 2008). These deposits are assumed to be at steady state before any temperature changes occur, and are not connected to active seeps. The top of the sediment column is an open boundary, allowing heat and mass transfer between the sediment and the ocean. The anticipated degree of warming and the time-temperature profiles vary greatly with location and model parameters (Figure 1, from Elliott et al., 2001), with the Arctic continental shelf experiencing warming of approximately 3 ˚C/100 yr off the north slope of Alaska, but as much as 6 ˚C/100 yr of warming in regions affected by northward-flowing ocean currents, such as the shallow Barents Sea or the Bering Sea shelf. Consequently, we restrict our representation of ocean warming to linear temperature increases of ΔT = 1, 3, 5, and 7 ˚C over a 100 yr period to describe the evolution of ocean temperature at the seafloor. Constant pressure (corresponding to a constant ocean water depth and salinity) is maintained at the top of

the sediment column, while the temperature at the top boundary (corresponding to the water at the ocean floor), is varied. We record methane fluxes and fluid flow velocities at the seafloor, as well as the pressure, temperature, and phase saturation profiles at regular intervals. The after 100 yr, the temperature is held constant (as predicting temperature changes beyond this point becomes increasingly speculative), and the system is allowed to evolve toward a new equilibrium for a total of 1,000 yr. We perform these simulations at regular depth intervals ($\Delta z \leq 25$ m) from 300 m down to 1000 m to assess the point-by-point potential for release across a wide range of bathymetry in the basins of interest. These simulations, although rough schematics of the wide range of possible hydrate depths, distributions, and saturations, allow a systematic examination of the many coupled processes that drive and regulate possible hydrate dissociation.

Results

The simulations performed as part of this basin-scale study cover a wide range of depth, temperature, and ΔT. To illustrate the process of dissociation, we present a select group of the most relevant results that go into the basin-scale integration.

Process of dissociation.

We first present an example of the properties of temperature-driven hydrate dissociation as a function of depth and location, using initial conditions representative of the Beaufort Sea shelf. Such dissociation simulations are performed at many depth/temperature locations to drive the basin-scale integration.

Figure 2 illustrates the process of top-down dissociation seen for cold, shallow hydrate systems subjected to warming on timescales of 100 yr, illustrating the variation of the dissociation process with deposit depth (with the indicated depth representing the depth of water above the overlying seafloor), through comparison of $t = +100$ yr 1-D snapshots for 350 m, 450 m, and 500 m water depth. In comparing the first and second panel, we see that a deposit subjected to the same warming (+3 ˚C) over the same time period but existing at 100 m greater depth has progressed far less along the dissociation pathway at the 100-yr milestone. Only approximately ~1 m of hydrate has dissociated, creating only a small region of free gas. However, the temperature change has propagated a significant distance into the formation, with an inverted T-gradient existing to a depth of -45 mbsf. The greater depth of the deposit results in a higher initial pressure and increased hydrate stability. In the third panel of Figure 2, we see that a deposit 50 m deeper, in 500 m of water, shows no sign of dissociation at $t = +100$ yr, despite that the temperature change has again propagated a significant distance into the sediments. These illustrations suggest that hydrate dissociation may be limited to a narrow range of deposit depths and temperatures.

Evolution of cumulative methane release.

To best capture the consequences of methane release, cumulative fluxes of methane vs. time, rather than fluxes, illustrate the true load on the ocean (and perhaps atmosphere) for a given warming/dissociation scenario. Figures 3 and 4 illustrate the potential cumulative fluxes of methane, V_{CH4}, into the ocean for various depth/temperature scenarios, using Beaufort Sea and Barents Sea conditions as an example. We present 1-D simulation results at 50 m or 100 m intervals to illustrate the changes seen during basin-scale integration.

In Figure 3, the cumulative methane fluxes, V_{CH4}, for a range of water depths is presented for two temperature scenarios (note the log scale for V_{CH4}). For a case of more significant warming, ΔT = +5 ˚C/100 yr, the cumulative methane released in aqueous and gaseous forms at 350 m water depth approaches 1000 mol/m^2 at the end of the first century of warming, and then methane release continues to evolve, reaching nearly 2500 mol/m^2 by the end of 300 yr. At 400 m depth, V_{CH4} approaches 1400 mol/m^2 after 300 yr, and at 450 m, 770 mol/m^2 at the same point in time. Cumulative fluxes decline significantly with depth, however, dropping to V_{CH4} = 330 mol/m^2 at 500 m and to only 4.6 mol/m^2 for systems in 550 m of water. Below 550 m, the amount of methane released is far less significant. Two effects are in play here—1) increasing water depth results in increased initial pressure, such that a higher temperature is required to destabilize the hydrate and 2) deeper systems have a slightly colder initial temperature (ranging from approximately 1.0 ˚C at 350 m-400 m depth to 0.5 ˚C below 550 m for the example of the Beaufort shelf). As a result, although the propagation of the temperature change proceeds at roughly the same pace for all systems, the dissociation of hydrate and the evolution of methane at the seafloor is reduced and delayed temporally. For 550 m depth, one may notice the rapid increase (over one order of magnitude) in V_{CH4} around t = +100 yr. This increase marks the arrival of free gas at the seafloor, at which point the flux transitions from primarily aqueous methane to primarily gaseous methane (also see Reagan and Moridis, 2008). For the systems at 600 m and 700 m, this transition does not arrive within the 300 yr timescale of the plots, and in fact, for 700 m, gas does not appear at the seafloor at anytime within the first 1000 yr.

For the case of more moderate warming, ΔT = +3 ˚C/100 yr (Figure 3, second panel), the distinction between the potentially unstable “shallow” region and the more stable “deep” region becomes more pronounced. Cumulative release profiles appear quite similar for systems at 350 m and 400 m depths, with only slightly reduced fluxes and a delay of about 20 yr in the appearance of significant methane at the seafloor for the 400 m case. Deeper cases exhibit notable reductions in V_{CH4}. A system at 450 m depth begins to evolve significant methane at the seafloor at t = +100 yr rather than t = +60 yr at this reduced ΔT, and the order-of-magnitude “surge” in V_{CH4} due to the appearance of gas at the seafloor does not occur until around t = +180 yr. Deeper systems now do not produce significant methane fluxes within the time period of interest. Also visible in the second panel is the lower flux for the 500 m vs. that at 550 m. Although the pressure is slightly higher at greater depths, increasing hydrate stability, it also results in high methane solubility, enhancing the transport of aqueous methane from the system during the initial stages of warming, enhancing methane transport in the period before the appearance of gas at the seafloor. Gaseous methane evolves in the 500 m system around t = +250 yr, however (note the upturn in V_{CH4}), and this results in the rapid increases in V_{CH4} for the 500 m case after that time. For ΔT = +5 ˚C/100 yr, this effect is overwhelmed by the earlier evolution of significant gaseous methane in the 500 m case.

Realistically, the expected ocean warming is not expected to be uniform at all locations and depths, as indicated in Figure 1. Shallower waters along the top of the continental shelves warm more than deeper waters down the continental slope. A more realistic estimate is to scale ΔT as a function of water depth, such that we can approximate the temperature regimes estimated by the coupled climate-ocean models. In Figure 4, we present two such scaled series of cumulative flux profiles vs. depth and ΔT. In the first panel, ΔT scales from ΔT = +5 ˚C/100 yr

at 350 m down to +1 ˚C/100 yr at 700 m and below, capturing a more extreme profile of temperature excursion on the expected upper limit of what might be seen in the Arctic basin. In the second panel, the variation is shallower, ranging from ΔT = +3 ˚C/100 yr at 350 m down to +1 ˚C/100 yr at 600 m (with 700 m and below showing no short-time temperature variation), more representative of the profile suggested by the IPCC A1B simulations (Figure 1). The first panel, the "strong warming" case, shows a strong separation between the "active" region—hydrates in water depths shallower than 500 m—and the less active, deeper systems with cumulative fluxes 2 to 3 orders of magnitude smaller. The combination of increased stability and a smaller warming signal at increasing depth drives this segregation. Similar to what is seen in the constant- ΔT evaluations, cumulative fluxes range from V_{CH4} = 30 – 1000 mol/m^2 after 100 yr of warming within the active zone, but drops below 0.1 mol/m^2 for deeper locations. At t = +300 yr, shallower locations may contribute 500 – 2500 mol/m^2 without significant additional methane from deeper locations. In the second panel, the "A1B" case, the shallower variation in ΔT leads to a less dramatic segregation between the active and less-active zones, but it is clear that only the shallowest—350 m and 400 m—cases contribute greatly to any large-scale methane release. The 450 m case shows that gas evolution is withheld until after t = 180 yr, and all deeper systems exhibit only small, aqueous releases of methane.

Another basin of interest is the Sea of Okhotsk, notable due to the active methane releases seen along the edge of Sakhalin Island, and due to the large estimated quantity of in-place shallow hydrates (via BSRs and heat flux estimates)—as much as 7 □ 10^{15} mol CH_4 (Ludmann and Wong, 2003). An interest feature of this basin is that the temperature profile below 400 m is roughly constant at 2 ˚C, with colder surface waters, but with a potential 2 ˚C - 6 ˚C of warming anticipated by the A1B simulations, mainly concentrated around the expected "active zone" around 350 m – 450 m. Figure 5 repeats the previous analysis of cumulative release vs. depth/temperature for deposits characteristic of the Okhotsk basin (Ludmann and Wong, 2003; Wallman 2006). Once again, we see a rapid decrease in cumulative methane release with increasing depth (first panel). Hydrates at shallow depths are both colder than in the previous case, due to the unusually shallow temperature gradient, and also more sensitive to temperature change relative deeper deposits, as the increase in pressure with depth is not balanced by an increase in temperature with depth. In the second panel, we see the cumulative release for a system where ΔT varies as a function of depth (A1B estimates for Okhotsk, i.e. Figure 1). Now, a large separation between "active" and "stable" zones is seen, with hydrates at 350 m – 400 m generating V_{CH4} = 90 – 1000 mol/m^2 CH_4 by t = 100 yr, but with deeper deposits producing only a small fraction of that total, likely only in the aqueous phase.

It is thus clear that, accounting for realistic depth/temperature effects, the most sensitive hydrate deposits under ocean temperature change scenarios will be located in a relatively narrow zone along continental margins, confined to regions where a combination of a strong warming signal and nearness to the edge of the GHSZ (a function of depth and initial temperature) leads to a plausible mechanism for rapid dissociation. Hydrates in the abyss are not likely to play a large role in short-term climate feedbacks. This narrow region is also likely to be the only source of large-scale fluxes of gaseous methane (which may form plumes, as seen off Spitsbergen, and transport methane into the water column in greater quantities) driven solely by local warming and hydrate dissociation, and therefore may be the only region where it is likely that the methane

can escape the various oxidation processes with any high probability and enter the water column efficiently.

Conclusions and Estimates

A basin-scale assessment of submarine hydrates in the arctic reveals a new, limited view of the possibility of a "clathrate gun" methane release event and its potential impact on the environment. The picture, as of the end of Year 3, is as such:

1) Sparse hydrates alone can release significant quantities of methane under the influence of moderate changes in the overlying water temperature. The release is controlled rather than explosive, due to the moderating influence of heat transfer through sediments, the endothermic nature of hydrate dissociation, and the limitations of gas transfer through marine sediments.
2) The release of methane at the seafloor due to warming of the overlying ocean is a function of initial temperature, depth of the water column above the hydrate-bearing sediments, and the magnitude and rate of temperature change.
3) These competing effects suggest that release of hydrate-derived methane due to ocean warming is likely to occur along a narrow "active" zone, beginning at the top of the GHSZ for a given water-column temperature regime and extending only to the point where increasing water pressure and decreasing water temperatures result in hydrate that is stable under the influence of expected temperature changes.
4) For submarine hydrate deposits along the arctic shelf, this region is likely to occur only from the shallowest possible extent of the GHSZ (about 320 m) to about 500 m, at which depth the combination of increasing pressure and decreasing temperature rapidly move any hydrate well into the stability zone.
5) The vast stores of hydrate methane in the deep ocean are likely to be stable for all expected climate-change scenarios.

The goal of this extended research project is to assess, quantitatively, the possible global consequences of the injection of hydrate-derived methane into the oceans and atmosphere due to expected changes in ocean temperature. In recently published research (Elliott et al., 2010; 2011) coupled ocean transport/methane biochemistry simulations establish that, under the conditions of hydrate-derived methane release, a considerable amount of methane could remain within the water column above and downcurrent from the release site as a consequence of research limitations—most notably, the lack of sufficient oxygen to feed the biological conversion of methane to CO_2. Such oxygen limitations both increase the potential for methane release into the atmosphere (important in that methane is a powerful greenhouse gas) and pose a heretofore-unanticipated biochemical impact on the ocean biosphere. The simulation work by Elliott et al. demonstrates that poorly ventilated basins, such as the sea of Okhotsk, could be severely impacted by the injection of 5.9×10^{12} mol CH_4 over a 30 yr period. Regions with more available oxygen, such as the Arctic Ocean, are more resilient to such releases, but significant methane plumes may form and persist, subjecting the local biological community to elevated methane concentrations and decreased oxygen concentrations.

From the edge of the Beaufort basin (north of Point Barrow) to the Queen Elizabeth Rise, approximately 1.4×10^9 m^2 of seafloor lies within the "active" zone for hydrate dissociation. Taking bathymetry data from the NOAA ETOP2 dataset (sampled at 40 min intervals), we can determine a rough estimate of the potential methane flux from each gridblock (specifying depth from bathymetry, and estimating T and ΔT as in the previous section, using the "cold" scenario in Figure 4) and sum these fluxes across the basin to determine the first "ballpark" estimate of the magnitude of hydrate-derived methane release. Assuming ubiquitous but sparse hydrate within the GHSZ may be overly optimistic and direct observation of shelf hydrates in the Beaufort has been limited, but we can use this assumption as an upper bound. This then leads to basin-wide cumulative release of $V_{CH4} = 2.6 \times 10^{12}$ mol CH_4 at $t = +30$ yr, $V_{CH4} = 5.2 \times 10^{13}$ mol CH_4 at $t = +100$yr, and a possible $V_{CH4} = 1.5 \times 10^{14}$ mol CH_4 after $t = +300$ yr from the onset of warming. These values are within a magnitude of the assumed net source term for the coupled ocean transport/chemistry studies in Elliott et al. (2011), which injected a total of 2.4×10^{13} mol CH_4 over a 60 yr period (measured from the onset of release, not warming) into the Beaufort basin (localized, however, at two points, one near Barrow and near the Queen Elizabeth Rise). Such injections resulted in localized methane plumes and corresponding localized reductions in dissolved oxygen, although for the well-ventilated Arctic Ocean waters, this alone is not enough to shut down methanotroph activity or create low-oxygen zones beyond the plume source itself.

However, a similar release (single point release) in a poorly ventilated basin such as the Bering shelf or the Sea of Okhotsk was shown have far more dramatic consequences, with ocean chemistry simulations suggesting rapid progress toward hypoxia and widespread transport of dissolved methane. Performing the same coarse integration of 1-D releases across the Sea of Okhotsk basin leads to somewhat somewhat sobering results. Adjusting the total hydrate occurance to only 80% of the existing GHSZ and using reported upper and lower estimates of saturations (all estimates from Ludmann and Wong, 2003), out simulations indicate an estimated input of 6×10^{12} mol CH_4 ($\pm 5 \times 10^{12}$) into the basin after 30 yr of release ($t = 83$ yr after onset of warming). This is very close to the 5.9×10^{12} mol CH_4 injected in the coupled simulations of Elliott et al. (2011) by $t = 30$ yr. Such a release, according to the POP simulations, results in significant reductions in oxygen in such a poorly ventilated basin (hypoxia, or perhaps localized anoxia). It is also important to note that such a release, while extremely significant in its biochemical consequences, only involves the dissociation of far less than 1% of the total estimated Okhotsk hydrate reservoir.

Once again, dissociation and methane release is confined to a narrow zone defined by depth/temperature considerations. Also, even if hypoxia is not a consideration elsewhere in the arctic, widespread increases in methane flux along the entire Arctic Ocean rim could eventually overwhelm the ability of the ecosystem to utilize the methane due to depletion of key nutrients (Elliott et al., 2010). As a result, continued analysis of the possibility of hydrate destabilization is warranted, with a particular focus on expanding the coupled modeling of dissociation to the global scale. The existing POP simulation work suggests about a 1% transfer of methane to the atmosphere via the sea surface, however, the POP simulator has received new bubble-plume parameterizations that are being used in the next generation of simulations to distribute methane more realistically throughout the water column, allowing transport of dissolved gases in the upper mixed layer and potential increases in the communication with the atmosphere.

References

Elliott, S.M., Maltrud, M., Reagan, M.T., Moridis, G.J., Cameron-Smith, P.J., "Marine Methane Cycle Simulations for the Period of Early Global Warming," *J. Geophysical Res. Biogeo*., 116, G01010, doi: 10.1029/2010JG001300, 2011.

Elliott, S.M., Reagan, M.T., Moridis, G.J., Cameron-Smith, P.J., "Geochemistry of Clathrate-Derived Methane in Arctic Ocean Waters," LBNL-3389E, *Geophys. Res. Lett.*, **37**, L12607, doi:10.1029/2010GL043369, 2010.

Ludmann, T, Wong, H.K., "Characteristics of gas hydrate occurrences associated with mud diapirism and gas escape structures in the northwestern Sea of Okhotsk," *Marine Geology,* **201**, 269-286, 2003.

Reagan, M.T. and G.J. Moridis, "Oceanic Gas Hydrate Instability and Dissociation Under Climate Change Scenarios," LBNL-62999, *Geophys. Res. Lett.*, **34**, L22709, doi: 10.1029/2007GL031671, 2007.

Reagan, M.T. and G.J. Moridis, "The dynamic response of oceanic hydrate deposits to ocean temperature change," LBNL-01026E, *J. Geophys. Res. Oceans*, **113**, C12023, doi:10.1029/2008JC004938, 2008.

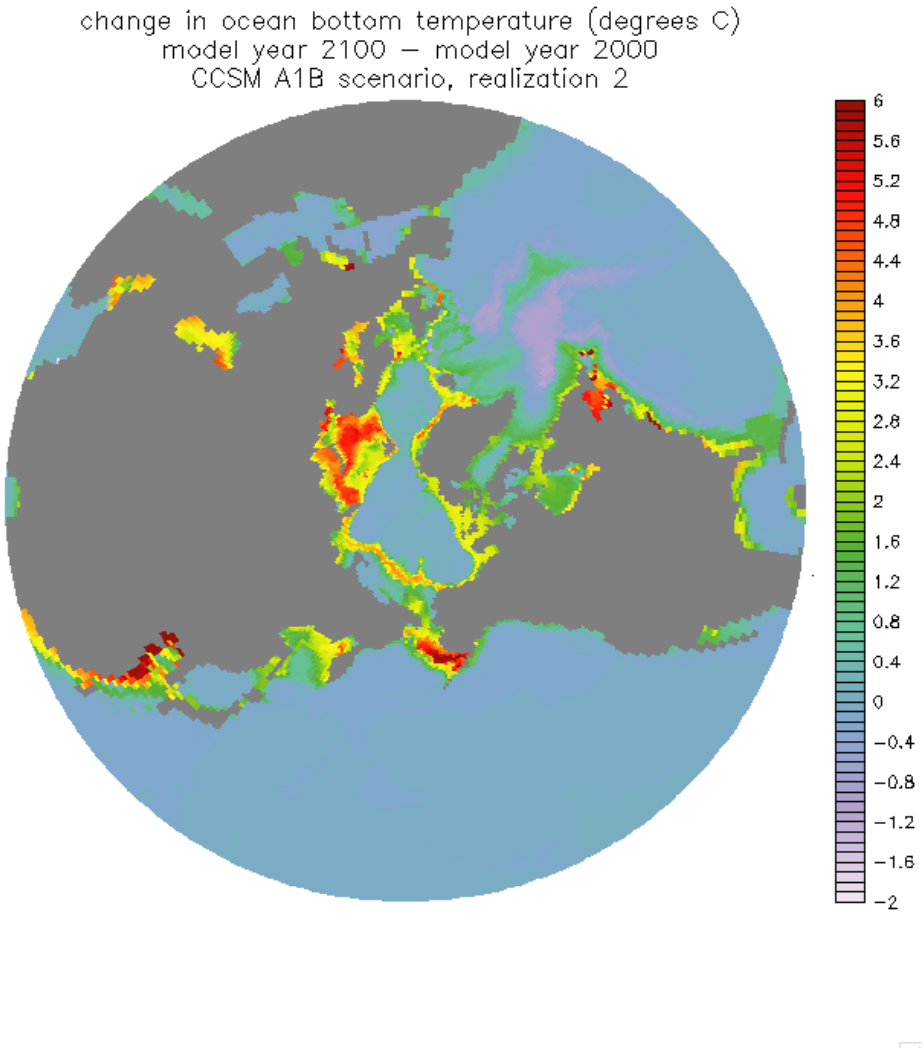

Figure 1. Anticipated ocean warming at the seafloor, for the IPCC A1B scenario for the years 2000-2100.

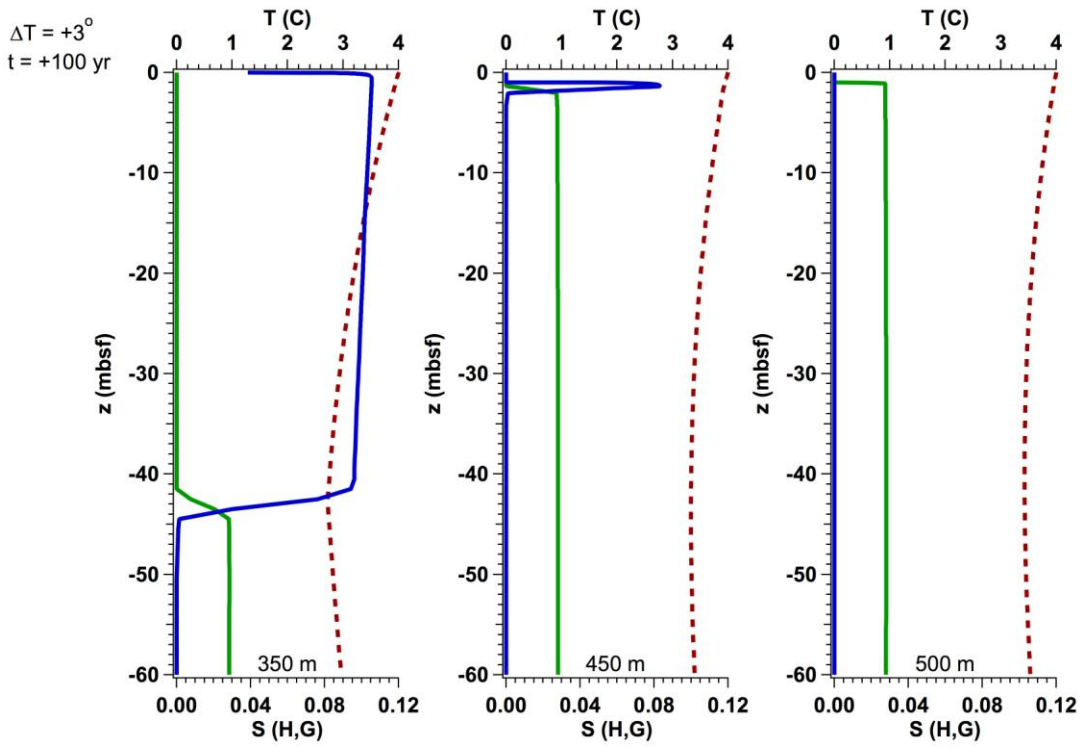

Figure 2. Dissociation of hydrate systems at 350 m, 450 m, and 500 m depth, subjected to +3 ˚C/100 yr warming, at t = +100 yr after the initiation of seafloor warming. The green line represents hydrate saturation, S_H, the blue line gas saturation, S_G, and the red line the temperature profile.

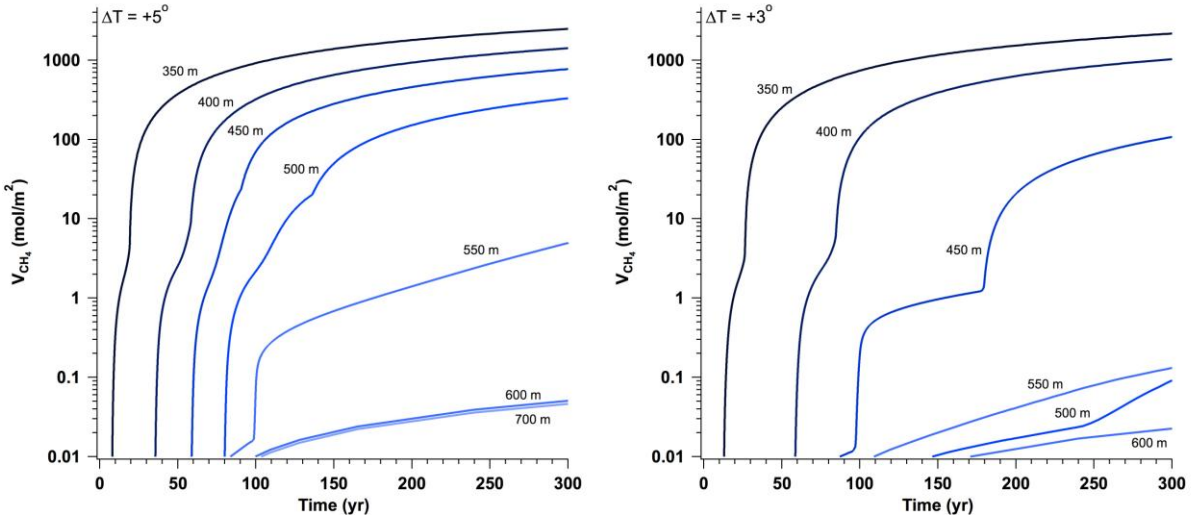

Figure 3. Cumulative fluxes of methane in gaseous and aqueous phases, V_{CH4}, at the seafloor for deposits where the seafloor is at 350 m to 700 m depth, for ΔT = +5 ˚C and +3 ˚C/100 yr. Note the log scale for V_{CH4}.

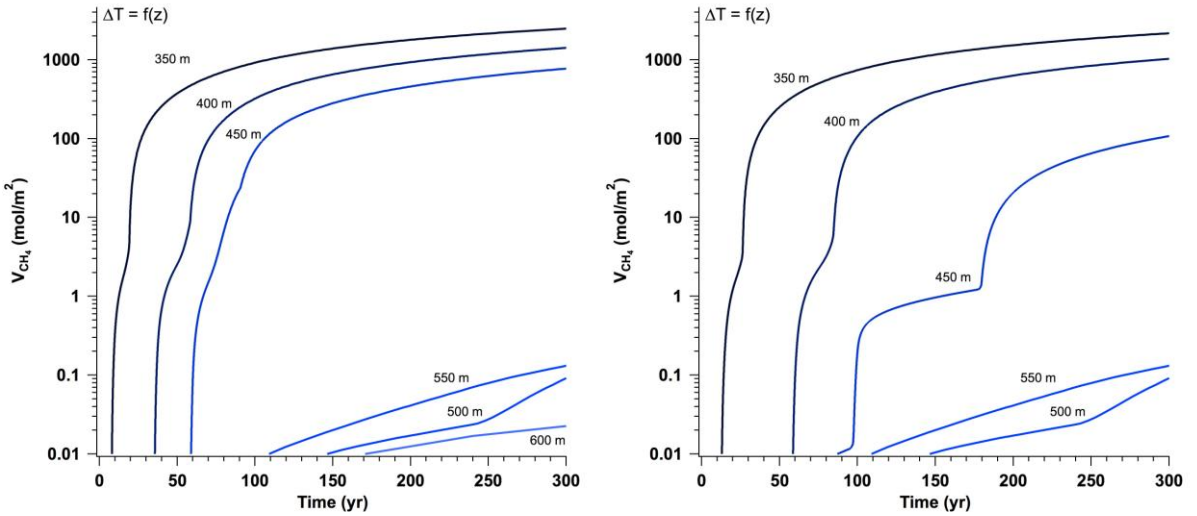

Figure 4 Cumulative fluxes of methane in gaseous and aqueous phases, V_{CH4}, at the seafloor for deposits where the seafloor is at 350 m to 600 m depth, with ΔT varying with depth. Note the log scale for V_{CH4}.

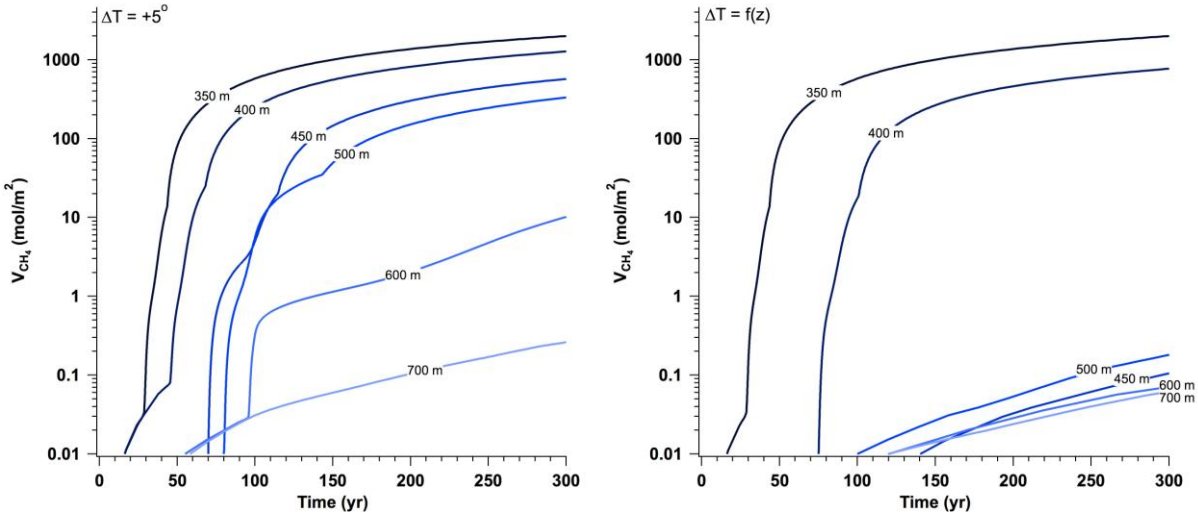

Figure 5 Cumulative fluxes of methane in gaseous and aqueous phases, V_{CH4}, at the seafloor for deposits in the Sea of Okhotsk where the seafloor is at 350 m to 700 m depth, with ΔT = +5 ˚C and with ΔT varying with depth. Note the log scale for V_{CH4}.